Developments of a 2D position sensitive neutron detector*

TIAN Li-Chao(田立朝)[1,2,3;1)] TANG Bin(唐彬)[1,3] WANG Xiao-Hu(王小胡)[3]
LIU Rong-Guang(刘荣光)[1,3] ZHANG Jian(张建)[1,3] CHEN Yuan-Bo(陈元柏)[1,3]
SUN Zhi-Jia(孙志嘉)[1,3;2)] XU Hong(许虹)[1,3] YANG Gui-An(杨桂安)[1,3] ZHANG Qiang(张强)[1,3,4]

[1] State Key Laboratory of Particle Detection and Electronics, Beijing 100049, China
[2] Graduate University of Chinese Academy of Sciences, Beijing 100049, China
[3] Institute of High Energy Physics, Chinese Academy of Sciences, Beijing 100049, China
[4] China University of Petroleum, Beijing 102249, China

Abstract: China Spallation Neutron Source (CSNS), one project of the 12th Five-Year-Plan scheme of China, is under construction in Guangdong province. Three neutron spectrometers will be installed during the first phase of the project, and two-dimensional position sensitive thermal neutron detectors are required. Before the construction of the neutron detectors, a prototype of a two-dimensional 200 mm×200 mm Multi-wire Proportional Chamber (MWPC) with Ar/CO_2 (90/10) flowing gas has been constructed. In 2009, the prototype was tested with the ^{55}Fe X-ray using part of the electronics, and performed well.

Following the test in 2009, the neutron detector was constructed with the complete electronics and filled with the 6 atm. ^{3}He+2.5 atm. C_3H_8 gas mixture in 2010. The neutron detector has been primarily tested with an Am-Be source. In this paper, new developments of the neutron detector including the design of the high pressure chamber, the optimization of the gas purifying system and the gas filling process will be reported. The results and discussion are also presented in this paper.

Key words: thermal neutron detector, two dimensional MWPC, Am-Be neutron source

PACS: 29.40.Cs, 29.40.Gx, 29.90.+r **DOI:** 10.1088/1674-1137/36/6/008

1 Introduction

Thermal neutron scattering techniques are playing an important role in diffraction experiments to determine molecular and crystal structures in biology, condensed state physics and polymer chemistry requiring high flux neutron sources. China Spallation Neutron Source (CSNS), as the first spallation neutron source in the developing countries, will be working at the beam power of 0.1 MW and the neutron flux of 2.0×10^{16} cm$^{-2}\cdot$s^{-1}. Three spectrometers will be installed during the first phase of the project. Efficient detectors with high position resolution, high detection efficiency and low gamma sensitivity are required for neutrons in the wavelength ranging from 1.8 Å to about 8 Å. Because of the high cross-section for neutron absorption (5330 b@1.8 Å), ^{3}He gas is widely used in many instruments [1–3]. The detector based on Multi-wire Proportional Chamber (MWPC) filled with ^{3}He gas can be built to a large size, with relatively good energy and position resolution, high efficiency and shows no radiation damage compared with the solid state and scintillation detectors.

Usually，to meet the characteristics of high neutron detection efficiency and high position resolution, the ^{3}He based neutron detectors work at a state of high pressure. The neutron detector consists of an MWPC and a high gas pressure container filled with the operating gas. To optimize the parameters of the MWPC and the main part of the neutron detector, and to guarantee that it can show excellent performance in neutron test, it is necessary to construct

Received 29 August 2011, Revised 18 October 2011
* Supported by National Natural Science Foundation of China (11127508)
1) E-mail: tianlc@ihep.ac.cn
2) E-mail: sunzj@ihep.ac.cn

a prototype of the MWPC and test it with flowing gas and X-rays. Good results were achieved in the X-ray test in 2009, after which a high pressure container was constructed and the MWPC was fixed in it. Later on, the operating gas was filled with good gas tightness and the neutron detector, equipped with complete electronics, was tested with the Am-Be source at the Institute of High Energy Physics (IHEP).

2 The MWPC prototype [4]

A prototype of a two-dimensional MWPC with atmospheric pressure and a flowing gas mixture of Ar/CO_2 (90/10) for X-ray had already been constructed prior to the neutron detector. The geometry of the two-dimensional MWPC is shown in Fig. 1. The MWPC, with a 200 mm×200 mm sensitive area, is of conventional design with a cathode plane, an anode plane and two orthogonal readout planes symmetrically located about the central anode plane. The cathode is made of a thin metal foil pasted on the window. The anode plane is made up of 15 μm diameter gold-plated tungsten wires (with the tension of 25 g per wire) with an inter-wire spacing of 2 mm. The X readout plane is made up of 50 μm diameter gold-plated tungsten wires (with the tension of 40 g per wire) with an inter-wire spacing of 1 mm. Every four wires are connected together to form one readout-strip. The direction of the readout wires is parallel to the anode wires. The Y readout grid is made up of 1.6 mm wide copper strips in the orientation orthogonal to the anode wires, with an inter-strip spacing of 2 mm. Every two copper strips are connected together to form one readout strip.

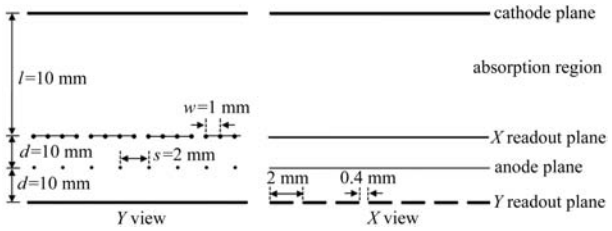

Fig. 1. Layout of the planes of the MWPC.

When an ^{55}Fe 5.9 keV X-ray entered a "Z" shape collimator, the detector got a clear image with an energy resolution (FWHM) of 23% shown in Fig. 2(a). The spatial resolution was tested through a 0.3 mm wide collimated X-ray beam. Considering the X-ray distribution as a uniform distribution after the collimator, the reconstructed position distribution along the anode wires is fitted with the convolution of the uniform and gauss distributions, which is showed in Fig. 2(b), and the σ of the gaussian distribution is 93 μm. So, the spatial resolution (FWHM) along the anode wires is about 220 μm. The successful construction of the prototype laid the foundation for the construction of the neutron detector.

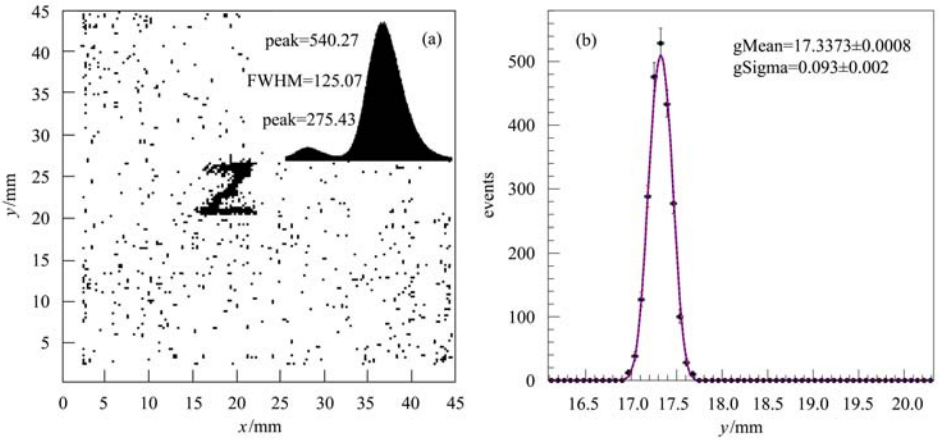

Fig. 2. Performance of the prototype. (a) imageing ability; (b)reconstructed position distribution.

3 Developments

The main structure of the thermal neutron detector is the same as the prototype (see Fig. 1). The neutron absorption by ^{3}He induces a fission reaction and emission of two charged particles, one triton and one proton, in opposite directions, with a total kinetic energy of 764 keV which induces the primary ionization in the gas. The position of the neutron is considered to be the centroid of the primary electrons associated with the nuclear reaction point. But actually the ionization centroid is displaced to the point of 0.4 times the proton moving range apart from the

nuclear reaction point [5]. To meet the characteristics of high neutron detection efficiency and high position resolution, the wire planes should be sealed in a high pressure chamber with 6 atm. ^{3}He as detection medium and 2.5 atm. C_3H_8 as stopping gas. The high pressure chamber was designed, the gas purifying system was updated and all the electronics were tested before the performance test with the Am/Be source.

3.1 High pressure chamber

As the chamber works under high pressure, all the wire planes were fixed in a high pressure container, which consisted of a circle front cover made of aluminum alloy 6061-T6 and a circle back-plate made of stainless steel (see Fig. 3). Double "O" shape rings were used to seal the container. A 9 mm thick window with an area of 210 mm×210 mm was constructed in the center of the front cover to minimize neutron scattering. The 25 mm thick back-plate provided structural rigidity under the maximum gas pressure of 10 atm. The anode and cathode signals were transferred to the readout electronics via flanges deployed on the back-plate. A gas purifying system, consisting of a pump and a filter, was also included, so as to guarantee the purity of the operating gas [6].

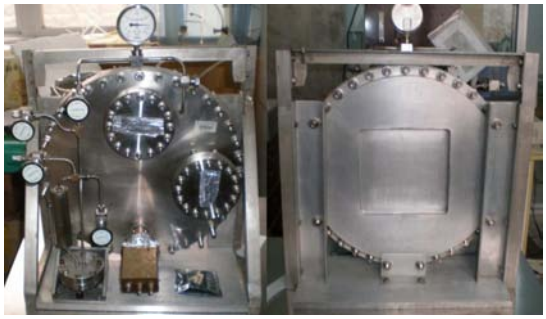

Fig. 3. The pictures of the high gas pressure chamber.

3.2 Gas filling

The gas purifying system was updated due to a small gas leakage, and the gas filling process was completed at Beijing Nuclear Instrument Factory in February, 2010. Some unnecessary tubes were removed to reduce the likelihood of gas leaking. To test the gas tightness, the chamber was filled with 9 atm. of ^{4}He gas and kept for about two months without obvious leakage. Before being filled with the operating gas, the chamber was first heated to 60 ℃ and evacuated until a stable vacuum was obtained (about 3×10^{-4} Pa, in order to release the residual gas in the materials. The vacuum state was kept for 48 hours, and then pure argon was flushed through the chamber for 5 hours, to remove any leftover gas in the chamber. Then, the chamber was evacuated to vacuum again. Finally, the chamber was filled with ^{3}He/C_3H_8 mixture. Fig. 4(a) shows the changes in gas pressure and temperature after the 8.5 atm. of operating gas was filled over 45 days. The fluctuation was caused by the temperature and the error comes from the reading of the pressure gauge. Fig. 4(b) shows the ratio of the calculated pressure, corrected by temperature, to the initial pressure in each day, which are within the accepted reading error limits.

Presuming it is an exponential leakage, the ratio changes with time as the function (1), so the leakage lifetime is $T_0 = 18 \pm 5.5$ years. This means that about 18 years later the gas pressure will be 1/e of the initial pressure. Since the C_3H_8 molecules are much larger than ^{3}He atoms, the main leaking gas will be ^{3}He. This means there will be effects on the detection efficiency and the gas gain as a function of the gas leaking, which are shown in Table 1, assuming the detector is working with the same high voltage. The numbers in the column of the Relative Gas Gain are the ratios of the gain at different time to that of the initial state.

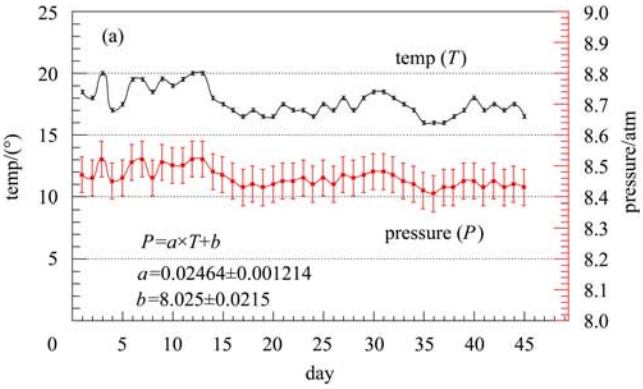

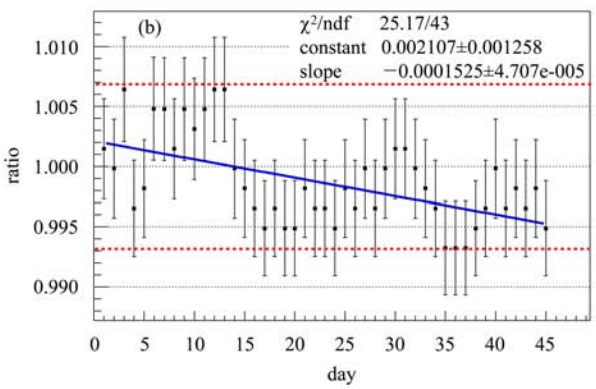

Fig. 4. Pressure variety of the Chamber. (a) Pressure and temperature varieties along time; (b) Ratio of the calculated pressure to the initial pressure.

Table 1. The effects on the detector performance caused by the gas leakage (simulated by Garfield [8] with the same high voltage).

elapsed time	detection efficiency	relative gas gain
initial state	75%	1
6 years ($T_0/3$)	59%±6.1%	196%±47%
9 years ($T_0/2$)	50%±9.4%	241%±43%

During actual running, the gas gain will increase and the gas pressure decrease at the same operation voltage [7]. To keep the stability of the gas gain, the operation voltage should be decreased over time. The neutron detection efficiency is decided by the two aspects, the neutron conversion efficiency and the detection efficiency of the electrons that are produced by the ^{1}H and ^{3}H. Since the neutron conversion efficiency will decrease sharply with the ^{3}He leakage, the neutron detection efficiency will decrease over time, although the electron detection efficiency will increase with the gas gain.

$$R = \mathrm{e}^{-0.0001525t+0.002107}, \quad (1)$$

where R is the ratio of the calculated pressure in future to the initial pressure and t is the time in unit of day.

3.3 Electronics

The location of the neutron is assumed to be the gravity center of the induced charges read out from the cathode strips. There are two aspects which should be taken into account during the electronic design. First of all, the detector should have a pretty good performance in n/γ discrimination. The γ rays can be discriminated from neutrons due to the differences of energy deposit in the gas. Secondly, we have to obtain the distribution of the induced charge on the cathode strips to get the center of gravity to reconstruct the position of the neutrons. A total of 100 individual position readout channels, 50 in each direction, and one anode readout channel are developed by the Electronics Group of IHEP. The total charge collected on the anode wire is used to get the energy loss information to trigger the readout. The analogue signal from the charge-sensitive preamplifier is directly converted to digital signals by a 10 bit 40 MHz FADC. Then the peak finding circuits based on FPGA, which can handle 16 channels at the same time, obtain the charge of each readout channel and deduct the baseline, and keep the results in a local buffer (see Fig. 5). All the electronics after the preamplifiers are built on the VME daughter card. The DAQ can read the buffer through the VME bus and save the raw data in a local hard disk for offline analysis. All the electronics have been calibrated together with the VME crate, which shows good long-term stability.

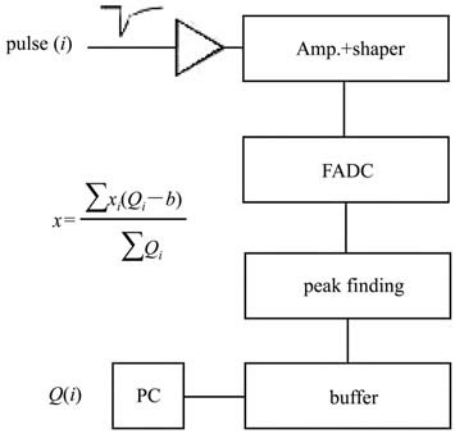

Fig. 5. Block diagram of the electronics.

4 Test with the Am-Be source

4.1 Experimental setup

The neutron detector was first tested with an Am-Be source, which was sufficient for uniform irradiation testing, but not powerful enough to generate collimated beams for high spatial resolution testing. The experimental equipment was set up as Fig. 6. In our experiment, the fast neutrons emitted from the Am-Be source were moderated through a 40 cm thick polythene block first and then went through a 12 mm thick Pb (as the shield of the gamma rays). Finally, the moderated neutrons entered the detector

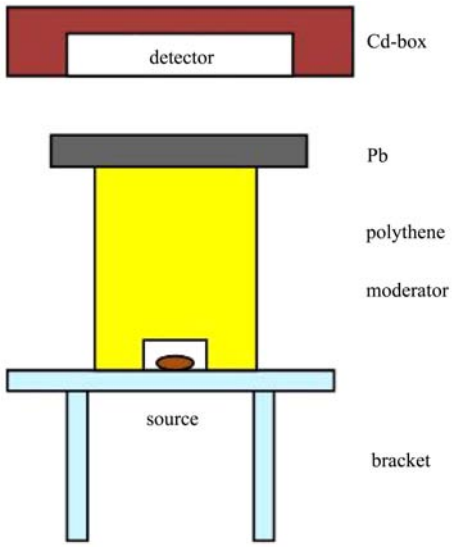

Fig. 6. The schematic map of the experimental equipment.

with a cadmium mask placed in front of the detector window. The whole detector was put in a Cd-box to absorb the surrounding thermal neutrons.

4.2 Results

1) Spectrum

The energy spectrum is the main basis in the n/γ discrimination. The energies deposited in the detector under different testing conditions are shown in Fig. 7. The spectrum (a) was tested with the ^{137}Cs gamma ray source; the spectrum (b) was tested with an Am-Be source with a moderator and Pb in front of the window shown in Fig. 6; the spectrum (c) was tested under the same condition with (b) but with 4 mm thick cadmium more in front of the window to absorb the thermal neutrons from the source. Three spectrums had been normalized by the run time. The peaks on the right side corresponded to the energy disposed by neutrons, while the middle ones near the 200 channel corresponded to the gamma rays. The left peak was caused by the fake triggers due to the electronic noise.

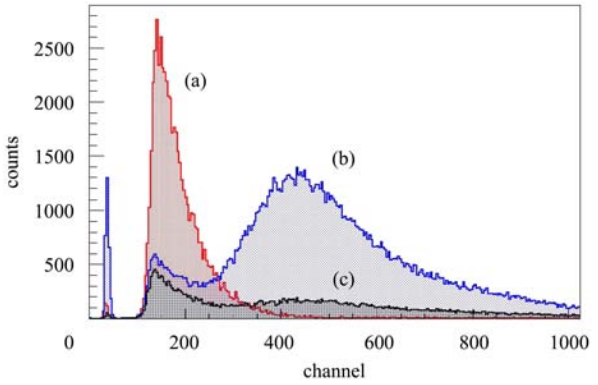

Fig. 7. Energy spectra under different test conditions.

With appropriate thresholds selected, the gamma rays could be discriminated from the neutrons easily through the comparison of the spectrum (a) with (b). But there were many upper-Cd neutrons and high energy gamma rays (together about 17% of the thermal neutrons) which could still penetrate the cadmium and be captured in the detector from the comparison of the spectrum (b) with (c). They were the main background in the thermal neutron test.

2) 2D imaging

A two-dimensional image was obtained by placing a mask (shown in Fig. 8(a)) in front of the detector's window. The mask with 2 mm thick was made up of a cadmium plane with a hole of the character "H". In order to get a sharp image we had to make the strokes of the character a little wider, due to the low intensity of the source and the high neutron scattering in the moderator. To collect enough neutron events the whole system had to take data for at least 10 hours. The charge collected on the anode, the number of fired strips, the maximum charge and the sum of the charge induced on fired strips were used to discriminate the gamma rays and neutrons in the analysis. This image (shown in Fig. 8(b)) could also illustrate the good uniformity of response.

3) The position linearity

The position resolution was tested in the direction parallel to the anode wires (Y direction) at variable positions. Due to the low flux of Am-Be source, only a rough position resolution about 4.9 mm (sigma) was achieved. The position linearity was tested and the fit function of the measured positions to the actual positions was $y = 1.0117x + 0.0811$. (see Fig. 9). The linear correlation coefficient was 0.9998, which shows a good linearity.

4.3 Discussion

The spatial resolution of the neutron detector is mainly determined by the proton moving range in the operation gas and the intrinsic position resolution of the MWPC. The proton moving range is determined primarily by the propane pressure - it is about

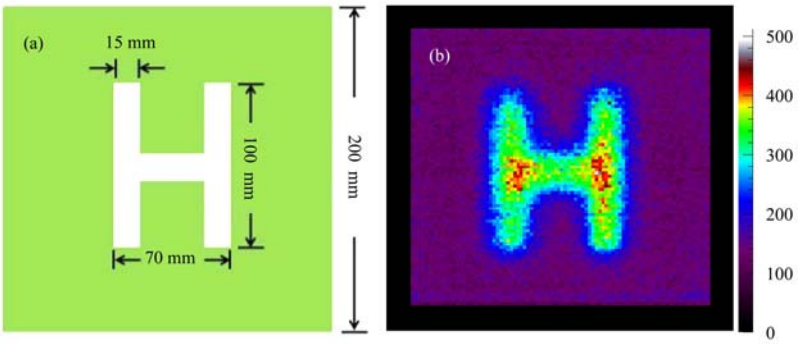

Fig. 8. 2D imaging ability. (a) "H" mask; (b) "H"image.

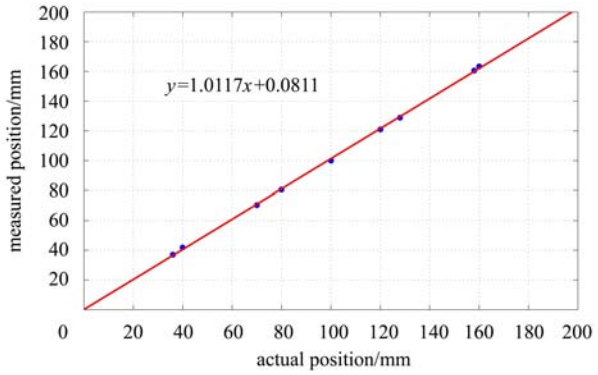

Fig. 9. The position linearity of the detector.

1.43 mm for our choice of 2.5 atm. from the SRIM [9] simulation. The approximate intrinsic position resolution of MWPC was 220 μm from the ^{55}Fe test. So, the theoretical neutron position resolution should be the square root of the quadratic addition of the error caused by the proton moving range and the intrinsic position resolution, which is better than 1.45 mm (FWHM) according to the Eq. (2).

$$\sigma_{\rm n} = \sqrt{\sigma_{\rm g}^2 + \sigma_{\rm i}^2}, \tag{2}$$

where $\sigma_{\rm n}$ is the theoretical neutron position resolution; $\sigma_{\rm i}$ is the intrinsic resolution from the X-ray test; and $\sigma_{\rm g}$ is the error caused by the proton moving range.

The reasons why the position resolution in our test is not as good as the expected result are as follows:

i) The high background.

The background, mainly the upper-Cd neutrons and high energy gamma rays from the surroundings, was too high, despite the detector being put in a Cd-box since there were other neutron sources and gamma sources in the lab. The signal to noise ratio was very low. The intensity of thermal neutron from the moderator was not high enough, so we had to take data for a long time.

ii) Hard to collimate the neutrons.

The neutrons through the moderator could be considered a plane source in front of the detector window since the neutron emitting direction, the angle between the emitting direction and the normal line of the detector's window were from about 0 to 90 degrees shown in Fig. 10. So, most of the thermal neutrons could not go into the detector perpendicular to the window, which made the edge of the character "H" not clear enough.

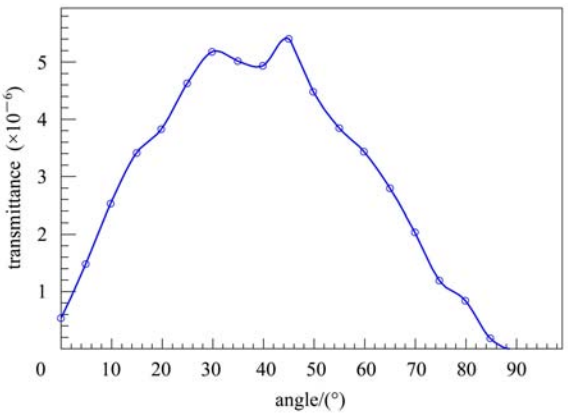

Fig. 10. The thermal neutron emitting angle distribution from the moderator (geant4 simulation result).

5 Conclusion

The two-dimensional thermal neutron detector has been constructed with a complete electronics system and filled with the 6 atm. ^{3}He+2.5 atm. C_3H_8 gas mixture in 2010. The leakage lifetime of the chamber is about 18 years after the updates of the gas purity system. The whole electronic system has good long-term stability. The detector has a good ability in n/γ discrimination. As for the low intensity Am-Be source, which was not powerful enough to generate collimated beams, only a 2D image was obtained with the position resolution of 4.9 mm in sigma. But good position linearity was also achieved. A much better spatial resolution is expected to be achieved on the collimated thermal neutron source where there are much higher flux thermal neutrons.

References

1 Knott R B, Smith G C, Watt G et al. Nuclear Instruments and Methods in Physics Research A, 1997, **392**: 62
2 YU B, Harder J A, Mead J A et al. Nuclear Instruments and Methods in Physics Research A, 2003, **513**: 362
3 SHAIKH A M, DESAI S S, PATRA A K. Pramana - J. Phys., 2004, **63**: 465
4 BOIE R A, FISCHER J, INAGAKI Y et al. Nuclear Instruments and Methods, 1982, **200**: 533
5 WANG Xiao-Hu, ZHU Qi-Ming, CHEN Yuan-Bo et al. Chinese Physics C (HEP & NP), 2008, **32**: 903
6 Radeka V, Schaknowski N A, Smith G C et al. Nuclear Instruments and Methods in Physics Research A, 1998, **419**: 652
7 XIE Yi-Gang et al. Particle Detector and Data Acquisition. First Edition. Beijing: Sciece Press, 2003. 73 (in Chinese)
8 Veenhof R. Garfield Help Pages. http://garfield.web.cern.ch/garfield/
9 Ziegler J F. The Stopping and Range of Ions in Matter, vol. 2-6, Pergamon Press, 1977-1985. http://www.srim.org